

Measurement of the Superconducting Energy Gap and Fermi Velocity in Single-Crystal Lead Films by Electron Tunneling*

G. I. Lykken,[†] A. L. Geiger,[‡] K. S. Dy, and E. N. Mitchell

Department of Physics, University of North Carolina, Chapel Hill, North Carolina 27514

(Received 1 April 1971)

The superconducting energy gap and reduced Fermi velocity have been measured as a function of crystallographic orientation by tunneling experiments using single-crystal thin films of Pb. Double gaps were observed in all directions except [100] in which a triple gap was found. Except in this last direction, the values measured agree with those of earlier experiments on bulk single crystals of Pb. Fermi velocities due to electrons from the second and third Brillouin zones are evaluated from a study of Tomasch oscillations in these films. Data are reported for the following orientations: [100], [110], [111], [211], and 5° off [100].

I. INTRODUCTION

It is the purpose of this paper to report experimental measurements of the superconducting energy gap and Fermi velocity in lead as measured in single-crystal films. These results will be compared with the results of other experimenters using in some instances similar, and in some instances different, techniques.

A. Gap Anisotropy

Studies of superconducting tunneling in single crystals were first performed by Zavaritskii¹ on bulk single crystals of tin. He observed considerable anisotropy (i. e., the value of the gap Δ_0 depended on orientation), and additionally observed multiple gaps (see Fig. 1, interval *a*) at many orientations. The value of Δ_0 varied by as much as 30% for different orientations. Bennett² has published a model for calculating the gap anisotropy in the ener-

gy gap due to the anisotropic variation of the phonon density of states. Treating band effects as a perturbation, he then calculated the dependence of the energy gap on the Fermi surfaces of the second and third Brillouin zones. From the calculated energy-gap anisotropy he predicted multiple gaps in the electron-tunneling characteristics.

The multiple gaps are, in general, a consequence of contributions to the tunneling current of electrons from the second (hole-surface) zone and third (electron-surface) zone. At least two distinct gaps were predicted for tunneling in [110] and [111] directions and three gaps in the [100] direction. The predicted values of $2\Delta_0$ encompassed a range of about 10% of the gap value.

Blackford and March³ measured the superconducting gap in bulk lead in several directions including the principal directions. In their experiment, junctions were formed by evaporating lead films onto specified faces of a lead single crystal after it had

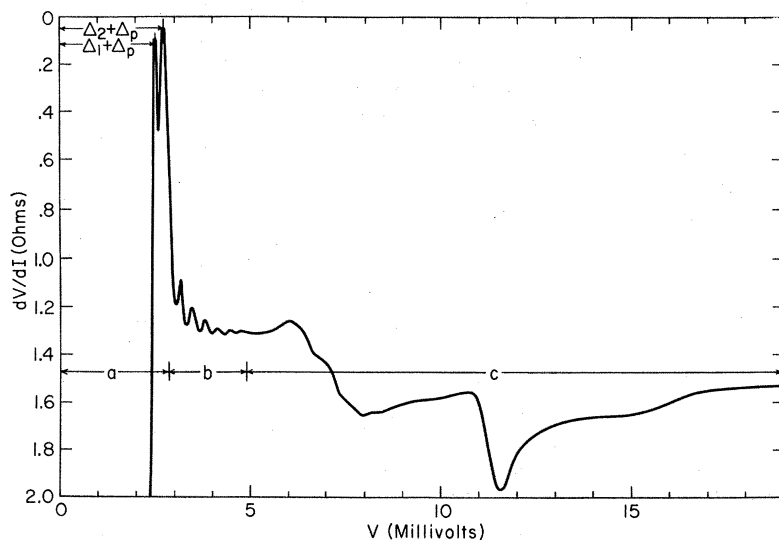


FIG. 1. dV/dI - vs- V characteristic for a lead-insulator-lead tunnel junction in which the bottom electrode is a 6.1- μ -thick [111] single-crystal film.

been oxidized on the surface and masked with Formvar. They found double gaps in all directions that they measured. In general, the gaps did not change as much with orientation (about 5%) as was the difference in the value of the two gaps in a given orientation (up to about 15%). The gap positions did not agree particularly well with values predicted by Bennett, though the relative positions of the gaps due to the hole conduction and electron conduction in a given direction agree with Bennett's predictions based on a comparison of relative current amplitudes in different orientations. Blackford and March did not see any evidence of the singularities arising from critical points in \vec{k} space as predicted by Bennett.

Wells *et al.*⁴ observed some anisotropy in the superconducting gap in aluminum thin films as a function of orientation. They found the anisotropy to be about one-half that predicted by Dynes and Carbotte.⁵ They did not see any multiple gaps and speculated that this was because their single-crystal films were too thin.

B. Tomasch Effect

Tomasch⁶ in 1965 first observed oscillations in the current and its derivatives (as a function of voltage) in the region beyond the energy gap (interval b in Fig. 1) in aluminum-insulator-lead tunnel junctions when examined at temperatures below the superconducting transition temperature of lead. It was found that this effect depended in a systematic way on the thickness of the lead film and could be related to the Fermi velocity in lead. McMillan and Anderson⁷ showed that this phenomenon could be explained as a simple quasiparticle interference effect caused by scattering from a perturbation $\delta\Delta$ in the energy-gap function on or near the film surfaces. They found that the effect caused the quasiparticle density of states to change by

$$\delta N(\omega) \propto \frac{\omega \Delta}{\omega^2 - \Delta^2} \delta \Delta \text{Si} \left(\frac{2Z(\omega^2 - \Delta^2)^{1/2}d}{\hbar v_F} \right), \quad (1)$$

where $\text{Si}(x) \equiv \int_x^\infty \sin y/y \, dy$, $Z(\omega)$ is the usual renormalization function in the Green's-function theory of superconductivity, and d is the thickness of the film. The Si function is an oscillatory function with maxima occurring when

$$n = \frac{Z(\omega^2 - \Delta^2)^{1/2}d}{\pi \hbar v_F}, \quad n = 0, 1, 2, \dots \quad (2)$$

McMillan and Anderson, by analysis of the voltage position of the extrema of these oscillations, determined the reduced Fermi velocity in the direction normal to the film surface. Using the data of Tomasch, they found the reduced Fermi velocity ($v_F' = v_F/Z$) in polycrystalline lead to be 0.98×10^8

cm/sec.

In a letter, the present authors⁸ reported preliminary measurements of the reduced Fermi velocity in or near the three principal directions which ranged in value $(0.93-1.37) \times 10^8$ cm/sec depending on orientation. This paper expands on the work, in that results for other orientations are presented, and reduced velocities for electrons from different zones in a given direction are reported.

II. EXPERIMENTAL METHODS

Single-crystal lead films were produced using variations of the procedures of Schober⁹ and Landry and Mitchell.¹⁰ Potassium bromide was cut with the normal to the face of the crystal in the same crystallographic direction as that desired for the normal to the film. The substrate was then polished, baked in air at 450 °C for thirty minutes, and upon cooling to 250 °C, was treated with water-saturated air until interference fringes were observed visually on the surface of the crystal.

The substrate was then placed in a standard oil-diffusion-pumped evaporator system and pumped to about 10^{-7} torr. The substrate was rapidly heated (in about ten minutes) to 200 °C, and a thin layer of silver (400–1500 Å) was rapidly deposited on the substrate. Immediately thereafter, lead was evaporated on the silver at a rate of about 1000 Å/sec. The quality of the films was relatively insensitive to the base pressure of the system. Equally good films were made in systems whose base pressure was 10^{-7} and 10^{-8} torr. The ambient pressure in these systems also differed by an order of magnitude.

It was found that the oxidation procedure was critical in the forming of the tunnel junction. Immediately after the formation of the film, it was cooled in vacuum to 150 °C. Oxygen was then admitted to the system until the pressure approached about 700 torr. When the substrate has further cooled to 75 °C, the temperature was stabilized, and the oxidation time extended as desired, depending on the impedance wanted for the junctions.

An oxidation time of thirty minutes yielded a junction of about 1 Ω (5×10^{-3} -mm² area), and ten hours yielded a junction of more than 10 Ω. After cooling to 30 °C, the system was opened, and the film covered by a second mask, and after reevacuation, a second lead film was deposited at rates about $\frac{1}{3}$ – $\frac{1}{10}$ that used for the initial film to a thickness of about $\frac{1}{10}$ the thickness of the first film. The underlying single crystal of lead could be reused by heating the film in vacuum to 150 °C and proceeding as before, though the impedance for comparable oxidation time increased by an order of magnitude. The authors feel that the success of this oxidation hinges on oxidizing the film surface before an ap-

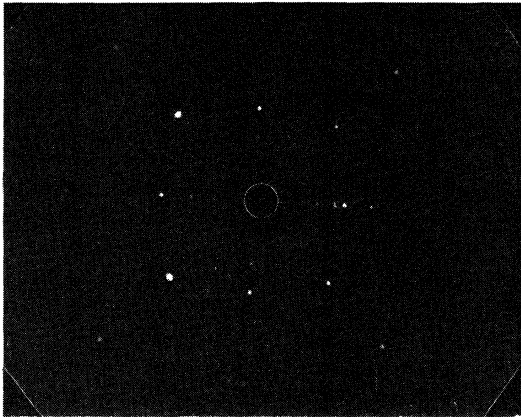


FIG. 2. X-ray back-reflection Laue pattern of a [100] single-crystal film of lead 8.4 μ thick.

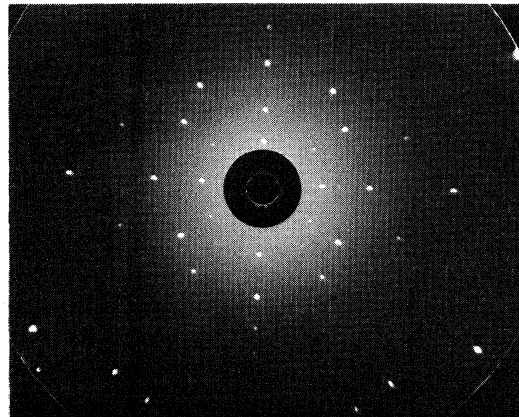


FIG. 4. X-ray back-reflection Laue pattern of a [110] single-crystal film of lead 7.0 μ thick.

preciable amount of oil from the vacuum system can condense on the substrate. Successful junctions were made about 80% of the time using this procedure.

Tunneling data were taken using circuitry similar to that described by Adler and Jackson.¹¹ The dynamic resistance dV/dI and its derivative d^2V/dI^2 were recorded as a function of bias voltage V . In addition, the gap structure was studied by recording dI/dV - and I -vs- V curves for the junctions. In all junctions used as data, the conductance inside the gap ($|V| < \Delta_1 + \Delta_2$) was at least two orders of magnitude less than outside the gap ($|V| \approx 3\Delta_1 + 3\Delta_2$). Gap structure, Tomasch oscillations, and phonon spectra were generally observed. Figure 1 shows a typical dV/dI -vs- V curve for one of these films exhibiting a double gap. Most of these data were taken at temperatures at or below 1.7 °K.

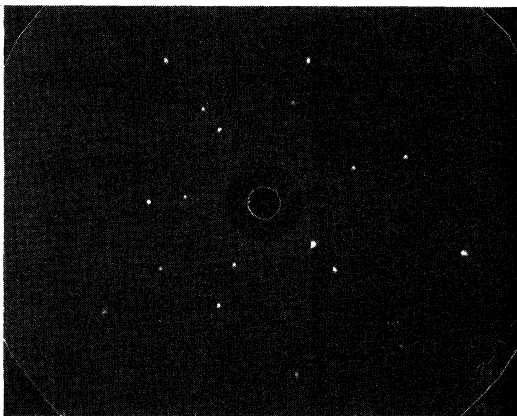


FIG. 3. X-ray back-reflection Laue pattern of a [111] single-crystal film of lead 7.3 μ thick.

The quality of the single-crystal films was evaluated by x-ray diffraction and electron diffraction. A General Electric x-ray machine with a tungsten-target x-ray tube was used to record back-reflection Laue patterns for these films. Typical exposures on medical x-ray film were 30 min with a 3-cm camera in which the anode current was 43 mA and the voltage was 20 kV. Typical patterns for the principal orientations are shown in Figs. 2-4. The underlying silver was evaluated on prototype samples using a Hitachi Model No. HU-11A electron microscope in a diffraction configuration.

No resistivity studies have been performed on these films to date. The underlying silver makes it necessary to do a two-step experiment in order to separate the behavior of the silver from that of the lead.

The thickness of the films was determined by weighing circular electrical contact pads of 3 mm diam which were at the ends of the single-crystal film strip. These were weighed using a Mettler direct-reading microbalance. It is estimated that the thickness could be determined to a precision of $\pm 5\%$ for the thinnest lead films, when one considers the uncertainties due to the mass of silver beneath the lead film, the measurement of the diameter of the pad, and gradation in the thickness of the film. The accuracy in the thickest specimens is probably not better than $\pm 3\%$.

III. RESULTS

About 100 successful junctions were made on a total of 74 films, and the data reported here represent results taken from about 40 single-crystal film tunnel functions.

A. Energy Gap

Table I shows a comparison of our results, those of Blackford and March,³ and the theory of Bennett.²

TABLE I. Comparison of gap data for this work, that of Blackford and March (Ref. 3), and the theory of Bennett (Ref. 2). In the latter case, multiple values are indicated as in his paper.

Orientation	$2\Delta_{\text{expt}}$	$2\Delta_{\text{BM}}$	$2\Delta_{\text{Bennett}}$
[110]	2.52 ± 0.02 2.74 ± 0.02	2.48 ± 0.01 2.76 ± 0.01	2.55, 2.71 (electron) 2.70 (hole)
[111]	2.36 ± 0.02 2.78 ± 0.02	2.36 ± 0.02 2.78 ± 0.02	2.58, 2.71 (electron) 2.77 (hole)
[100]	2.32 ± 0.02 2.56 ± 0.02 2.80 ± 0.02	2.44 ± 0.01 2.74 ± 0.01	2.60, 2.75 (electron) 2.86 (hole)
5° off [100]	2.47 ± 0.02 2.75 ± 0.02		
[211]	2.45 ± 0.02 2.78 ± 0.02	2.44 ± 0.01 2.78 ± 0.01	

On the basis of our experience, resolution of more-complex gap structures (and observation of Tomasch oscillations) depends on a relatively thin oxide (as witnessed by a low-impedance tunnel junction), since very-high-impedance junctions generally do not show multiple gaps or Tomasch oscillations. This is true, though the underlying crystal is evidently (from diffraction studies) as good quality as those in which multiple gaps are seen. This is most clearly portrayed when a film which has shown multiple gaps is reoxidized to higher impedance with an accompanying disappearance of multiple gaps and Tomasch oscillations. An example of this change is shown in Fig. 5. At least two possible explanations exist for this phenomenon. The thicker oxide may simply wash out some of the gaps, due to a reduction in the fraction of the electrons tunneled without scattering in the barrier. Alternatively, the difficulty might be due to alteration in the composition of the top layer of the lead during oxidation (e.g., formation of oxides and nitrides in the interior, rather than on the top, surface of the film). This would be consistent with MacVicar and Rose's observations¹² that multiple gaps cannot be seen in dirty single crystals of niobium.

Two different widths of films were used in these experiments. The single-crystal films were either 75 or 1500 μ wide. In the latter instance, the edges of the films were masked by evaporating MgF_2 over the edges to reduce the effective junction width to 440 μ . The overlay film was 75 μ wide in all instances. No difference in the tunneling characteristics could be discerned between the junctions with masked edges and those without masked edges, leading the authors to believe that none of the results reported here can be attributed to edge effects.

As in the work of Blackford and March,³ we have identified the gap with the minimum in dV/dI vs V (see Fig. 1). It should be noted that where Black-

ford and March³ identified gaps with given zones on the basis of the relative amplitudes of the contributions to the current in given directions, the same criterion could not be used here, since the relative magnitude of the current associated with the two gaps was not constant for different junctions made with films of the same orientation.

Our results (shown in Table I), in general, agree very well with the findings of Blackford and March, except in the [100] direction. Not only are the values of the gaps not in agreement in the [100] direction, but the number of gaps reported here is different. An example of the gap structure seen in the [100] direction is shown in Fig. 6. It is worthy of note that the values of the gaps seen by Blackford and March agree better with the values we observe at 5° off [100]. A more recent article by Blackford¹³ indicates a much wider range of values for the gaps in the [100] direction than earlier reported, but still only indicates two gaps. The smaller gap value remains 2.44 meV but the larger gap varies from 2.74 to 2.88 meV. The difficulty may be due to an inability on their part to resolve the three gaps and/or a strong orientational dependence of the value of the gaps in the [100] direction. This last point would be supported by the considerable

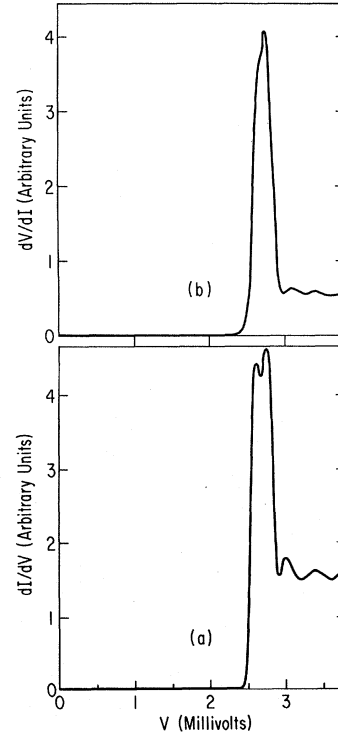


FIG. 5. dI/dV -vs- V curves for lead-insulator-lead tunnel junctions with a 3.5- μ -thick [110] lead film: (a) original junction; (b) second junction made with same single-crystal film of lead after it had been reoxidized in pure O_2 for 2 hours at 150°C.

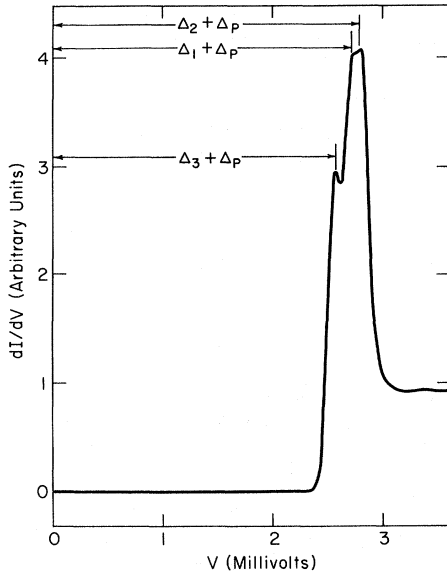


FIG. 6. dI/dV -vs- V curve for a junction in which the bottom electrode is a $6.7\text{-}\mu$ -thick [100] lead film.

difference seen here between [100] values and 5° off [100] values.

A satisfactory comparison with Bennett's² predictions is generally a bit more tenuous, as can be seen from Table I. We seem to be able to resolve as many gaps as he predicts. This is true even in the [110] and [111] directions, since gap values predicted by him in some instances overlap between zones 2 and 3. Furthermore, the relative values of the gaps found here and predicted by him can be made to agree with regard to zone identification in the [110] and [111] directions though *this is not unique*. However, the values he predicts are, in general, compressed into a smaller range than we observe. In agreement with Blackford and March,³ we observe none of the singularities predicted by Bennett associated with critical points in \mathbf{k} space.

B. Fermi Velocity

Tomasch oscillations have been observed in the majority of the junctions used as a basis of the gap determinations reported above.

Figure 7 shows an example of single sets of Tomasch oscillations in the tunneling characteristics of a $6.1\text{-}\mu$ Pb film (oriented in the [111] direction). The index n corresponds to minima in dV/dI .

These data could be analyzed using the formulation outlined in the introduction of this paper. Recently, alternate formulations have been presented by Wolfram¹⁴ and McMillan¹⁵ which give a more detailed account of the Tomasch effect. Instead of Eq. (1), we shall use McMillan's result for the

special case of a superconductor backed by a normal metal:

$$\delta N(\omega) \propto \text{Re}[(\omega - \Omega/\Omega) e^{-2iZ\Omega/\hbar v_F}], \quad (3)$$

where $\Omega = (\omega^2 - \Delta^2)^{1/2}$, and the rest of the symbols are as defined in Eq. (1). Using Eq. (3), the extrema condition for $\delta N(\omega)$ remains the same as (2). We shall assume that the dominant contribution to the oscillations in dI/dV is proportional to $\delta N(\omega)$ evaluated at $\omega = V - \Delta_p$, where Δ_p is the energy gap associated with the top layer of polycrystalline lead and V is the bias voltage. This assumption suffices as far as determining the extrema in the oscillatory term is concerned. A detailed study of the amplitude of the oscillations, on the other hand, would require a numerical computation of the integral which gives $I(V)$; this type of analysis will not be attempted here. In order for our curve to satisfy Eq. (3), we also have to correct for the dependence of Z on ω ; this is done by plotting n versus $Z(\omega) (\omega^2 - \Delta^2)^{1/2} / Z(\Delta)$, which is shown in the inset curve in Fig. 7 as a solid curve.

Not all data were as simple as that represented in Fig. 7, as can be seen in Fig. 8, where dV/dI

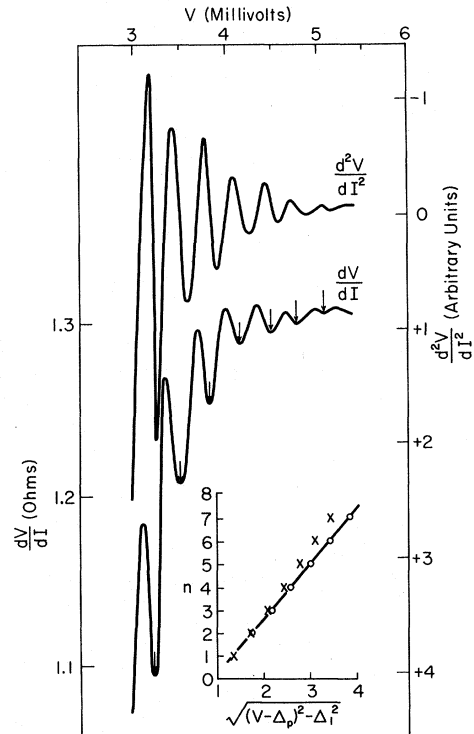


FIG. 7. Tomasch oscillations in the dynamic resistance and its voltage derivative for the junction of Fig. 1. Upper curve: d^2V/dI^2 vs V , scales top and right. Lower curve: dV/dI vs V , scales top and left. Inset curve, oscillation minima n vs $[(V - \Delta_p)^2 - \Delta_1^2]^{1/2}$; crosses are original data, while circles have been corrected for $Z(V)$ dependence.

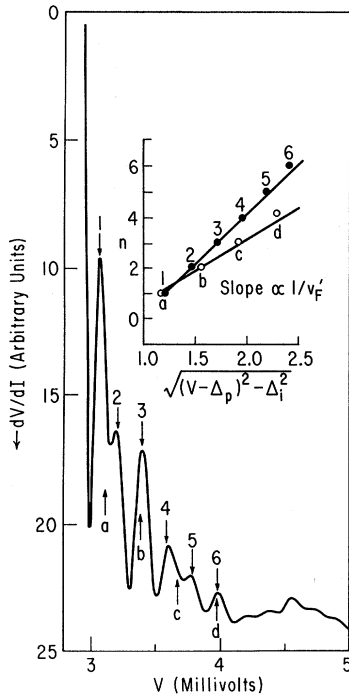


FIG. 8. dV/dI -vs- V curve for a junction in which the bottom electrode is a 4.9- μ -thick [110] single-crystal film. Inset curve shows a plot of oscillation minima n for damped sinusoidal oscillations of two different frequencies vs $[(V - \Delta_p)^2 - \Delta_i^2]^{1/2}$. Minima of the high-frequency oscillation, which in this figure is assumed to be associated with $2\Delta_2 = 2.74$ mV, are labeled by numbers 1-6; minima of the low-frequency oscillation, associated with $2\Delta_1 = 2.52$ mV, are labeled by letters a-d.

and d^2V/dI^2 as a function of V are plotted for another film oriented with the [110] direction normal to the film surface. This type of structure was only seen in junctions where the single-crystal film was thinner than about 5μ . In these cases, the oscillations can be interpreted as the superposition of two series. Tomasch¹⁶ has reported the observation of double series whose extrema fall on one straight line, such as the one in Fig. 7, provided the extrema of one of the series is indexed by half-integers. One explanation of this phenomenon is that the two series are due to quasiparticles having the same Fermi velocity, but are reflected by regions whose $\delta\Delta$ have opposite signs. The more detailed theory of Wolfram also predicts such a result. The double series reported here are of a different nature in that their extrema can be indexed only by two different straight lines, as can be seen in Fig. 8. This seems to imply the presence of carriers with two different Fermi velocities, which is consistent with Fermi-surface studies of lead and Bennett's² calculation that the tunneling current consists of holes and electrons

from the second and third Brillouin zones of single-crystal lead.

To test this model, an attempt was made to synthesize the experimental conductance in the region of the Tomasch oscillations (3-4.5 mV) by a superposition of two terms of the form given in Eq. (3):

$$\frac{dI}{dV} \propto A \left(\frac{V - \Omega_1}{\Omega_1} \right) \cos(K_1 \Omega_1 + \theta_1) + B \left(\frac{V - \Omega_2}{\Omega_2} \right) \times \cos(K_2 \Omega_2 + \theta_2) + V^2/\Omega_2^2. \quad (4)$$

In this expression, $\Omega_i = [(V - \Delta_p)^2 - \Delta_i^2]^{1/2}$, $K_i = 2 \text{Re}Z(\omega)\Omega_i d/\hbar v_{Fi}$, and A , B , θ_1 , and θ_2 are constants which are adjusted to give the best fit of this expression to the experimental curve. K_1 and K_2 , as well as A and B , could be approximated by inspection of the dV/dI curve in most cases. By trial and error, the above parameters, along with θ_1 and θ_2 , were varied until a reasonable fit was obtained.

An example of the results of this procedure is shown in Fig. 9. The basic form of the periodic structure is seen to be reproduced by this method, although the attenuation of the structure with energy is considerably less rapid than observed in the data. This is partly because the imaginary part of Z in

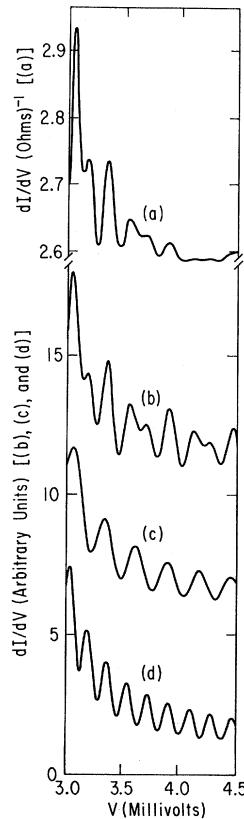


FIG. 9. Synthesis [curve (b)] of measured dI/dV vs V [curve (a)] for the junction of Fig. 8 by a superposition of two oscillations of different frequencies [curves (c) and (d)] as described by Eq. (4).

TABLE II. Comparison of measured values of the Fermi velocity to those derived from a four-parameter model where a and b correspond to the different positions on the electron surface as shown in Fig. 10(b). Values of Δ_1 and Δ_2 for each zone are given in Table I.

Orientation	$(v_F/Z)_{\text{expt}}$ (10^8 cm/sec)		$(v_F/Z)_{\text{Four-parameter}}$ (10^8 cm/sec)	
	Δ_1	Δ_2		
[110]	0.60 ± 0.05	0.61 ± 0.05	0.49	(hole)
	0.93 ± 0.05	0.96 ± 0.05	$0.36,^a 0.55^b$	(electron)
[111]	0.59 ± 0.15	0.62 ± 0.15	0.76	(hole)
	1.15 ± 0.10	1.20 ± 0.10	$0.39,^a 0.41^b$	(electron)
[100]	0.68 ± 0.10	0.70 ± 0.10	0.66	(hole)
	1.04 ± 0.05	1.07 ± 0.05	$0.24,^a 0.55^b$	(electron)
5° off [100]	0.72 ± 0.10	0.77 ± 0.10		
	1.37 ± 0.10	1.43 ± 0.10		

Eq. (3) is neglected in Eq. (4). $\text{Im}Z$ introduces a second energy-dependent term due to a decrease in the mean free path because of phonon emission. $\text{Im}Z$ is zero at Δ_0 , and increases with increasing energy,¹⁷ thus causing the oscillatory terms to be damped more rapidly with increasing energy. Upon consideration of impurity scattering in the film, Maki and Griffin¹⁸ have reported an additional term in the argument of the cosine function of Eq. (3) which may be slowly varying with energy; these terms are accounted for in the θ terms in Eq. (4). The K_1 and K_2 determined by this method were used to calculate two values of v_F/Z ; these were tentatively assumed to be due to electrons from two different Brillouin zones. The higher value of v_F/Z was always close to the value obtained for the same crystal orientation when only a single oscillation was seen.

Table II presents a summary of the results found here and the reduced Fermi velocity as calculated from the Anderson and Gold¹⁹ four-parameter model for the Fermi surface of lead. The renormalization constant Z has been taken from the data of McMillan and Rowell¹⁷ to be 2.33. The regions of the Fermi surface where v_F has been calculated were those assumed by Bennett,² and are shown in Fig. 10.

In both cases of single and double sets of oscillations, there is an uncertainty as to which of the gap values, Δ_1 or Δ_2 (see Fig. 1), to use in the calculation of v_F/Z . Values of v_F/Z derived by using both Δ_1 and Δ_2 are presented in Table II. The poor agreement of our measured values of v_F , compared to the calculated ones, prevents the association of any of the experimental values with a particular zone.

It was not possible to reduce the Tomasch oscillations observed in the [100] directions for those cases in which films thinner than 5μ were used, and three gaps were observed. Hence, no value for v_F/Z is given for the electrons contributing to

the gap whose value is $2\Delta = 2.32$ meV. It is of interest to note that v_F/Z (like the value of 2Δ) seems to change very rapidly near the [100] direction.

IV. SUMMARY

In this experiment, the superconducting energy gaps and the reduced Fermi velocity have been measured as a function of crystallographic orientation. Multiple gaps have been found in all orientations investigated. In all orientations where comparison of the gaps can be made with the data of Blackford and March,³ the results agree, except for the [100] direction. In this case, we see a triple gap as opposed to their double gap, and the values are different. Comparisons with Bennett's² calculations agree qualitatively in that we see the same number of resolved gaps in each direction, as is predicted by him. The values of the gaps do not agree in all cases, however, and we see none of the singularities predicted by him.

The values of the Fermi velocity derived from Tomasch-oscillation measurements lead to several interesting results. In some films, beats in the Tomasch oscillations were observed which can be interpreted as the superposition of two series of oscillations. Complicated structure in the Tomasch oscillations have previously been reported by Rowell and McMillan.²⁰ They observed complications in the oscillations only at lower voltages, and analysis by them of their data suggests that the complications are probably due to a distribution of Fermi velocities. In the present experiment, beats are clearly observed at higher voltages, and analysis of the data suggests a second distinct velocity.

It is further observed that in the junctions where beats were present, reoxidation of the junctions does not cause the beats to disappear. On the other hand, the presence of beats seems to depend strongly on the thickness of the film. A systematic study of the dependence of the relative amplitude of oscillations on the thickness of the film is clearly in order. An explanation for the beats could be the presence in the tunneling currents of carriers with two different Fermi velocities. This is pos-

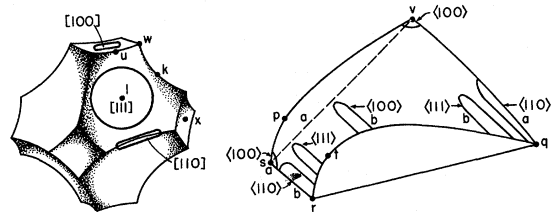


FIG. 10. (a) Second-zone hole surface with areas shown that contribute to tunneling in the three main symmetry directions. (b) Section of the third-zone electron surface with the areas shown that contribute for tunneling in the three main symmetry directions (from Ref. 2).

sible, for example, if the carriers come from two distinct portions of the Fermi surface. Bennett² has studied the region of the Fermi surface of lead which contributes to the tunneling current in the [110], [111], and [100] directions (Fig. 9). Using this information and the Anderson and Gold four-parameter model for the Fermi surface of lead,

the Fermi velocities of the different components in the tunneling current were computed. The results do not agree at all well with the measured values. In particular, one component has a velocity about twice the value of any of the computed ones. This discrepancy remains unexplained and is worthy of further study.

*Work supported by the U. S. Air Force Office of Scientific Research under Grant No. AF-AFOSR-1241-7 and by the Advanced Research Projects Agency of the Department of Defense to the University of North Carolina, Chapel Hill, N. C. 27514.

[†]Present Address: Physics Department, University of North Dakota, Grand Forks, N. D.

[‡]Present Address: Physics Department, University of Idaho, Moscow, Ida. 83843.

¹N. V. Zavaritskii, *Zh. Eksperim. i Teor. Fiz.* **45**, 1839 (1963) [*Sov. Phys. JETP* **18**, 1260 (1964)].

²A. J. Bennett, *Phys. Rev.* **140**, A1902 (1965).

³B. L. Blackford and R. H. March, *Phys. Rev.* **186**, 397 (1969).

⁴G. L. Wells, J. E. Jackson, and E. N. Mitchell, *Phys. Rev. B* **1**, 3636 (1970).

⁵R. C. Dynes and J. P. Carbotte, *Physica* (to be published).

⁶W. J. Tomasch, *Phys. Rev. Letters* **15**, 672 (1965).

⁷W. L. McMillan and P. W. Anderson, *Phys. Rev. Letters* **16**, 85 (1966).

⁸G. I. Lykken, A. L. Geiger, and E. N. Mitchell,

Phys. Rev. Letters **25**, 1578 (1970).

⁹T. Schober, *J. Appl. Phys.* **40**, 4658 (1969).

¹⁰J. D. Landry and E. N. Mitchell, *J. Appl. Phys.* **40**, 3400 (1969).

¹¹J. G. Adler and J. E. Jackson, *Rev. Sci. Instr.* **30**, 1049 (1966).

¹²M. L. A. McVicar and R. M. Rose, *J. Appl. Phys.* **39**, 1721 (1968).

¹³B. L. Blackford, *Physica* (to be published).

¹⁴T. Wolfram, *Phys. Rev.* **170**, 481 (1968).

¹⁵W. L. McMillan, *Phys. Rev.* **175**, 559 (1968).

¹⁶W. J. Tomasch, in *Tunneling Phenomena in Solids*, edited by E. Burstein and S. Lundquist (Plenum, New York, 1969).

¹⁷W. L. McMillan and J. M. Rowell, in *Superconductivity*, edited by R. D. Parks (Marcel Dekker, New York, 1969).

¹⁸K. Maki and A. Griffin, *Phys. Rev.* **150**, 356 (1966).

¹⁹J. R. Anderson and A. V. Gold, *Phys. Rev.* **139**, A1459 (1965).

²⁰J. M. Rowell and W. L. McMillan, *Physica* (to be published).

Quantized Flux States of Superconducting Cylinders*

William L. Goodman, Wayne D. Willis, Daniel A. Vincent,
and Bascom S. Deaver, Jr.

Department of Physics, University of Virginia, Charlottesville, Virginia 22901

(Received 30 April 1971)

We have measured the magnetic flux trapped in hollow superconducting cylinders (14–56- μ i.d., 0.1–5- μ walls, 0.5–2.5 cm long) as a function of the applied magnetic field in which the cylinder was cooled through its transition temperature. For most applied fields, the entire cylinder is in the same quantum state; for some fields there is a mixed state with bands along the cylinder in states differing by one flux quantum. In cylinders with walls thick with respect to the penetration depth, the trapped flux is an integral multiple of $hc/2e \pm \frac{1}{2}\%$. We have measured the temperature dependence of the trapped flux in a cylinder containing a single flux quantum and find a continuous reversible change by just the amount required to maintain the constancy of the fluxoid.

I. INTRODUCTION

London introduced the concept of the fluxoid Φ defined for any closed path within a superconductor by

$$\Phi = \oint (4\pi\lambda^2/c) \vec{j} \cdot d\vec{s} + \oint \vec{A} \cdot d\vec{s} = n\Phi_0, \quad (1)$$

where λ is the penetration depth, \vec{j} the supercurrent density, and \vec{A} the magnetic vector potential, and he predicted that Φ would be quantized.^{1,2} This prop-

erty of superconductors follows immediately from requiring that the macroscopic wave function be single valued. The quantum Φ_0 determined experimentally and related to the pairing of electrons by the microscopic theory is

$$\Phi_0 = hc/2e = 2.07 \times 10^{-7} \text{ G cm}^2. \quad (2)$$

For a hollow superconducting cylinder with wall thickness large compared to the penetration depth, a path can be chosen along which the current is ar-

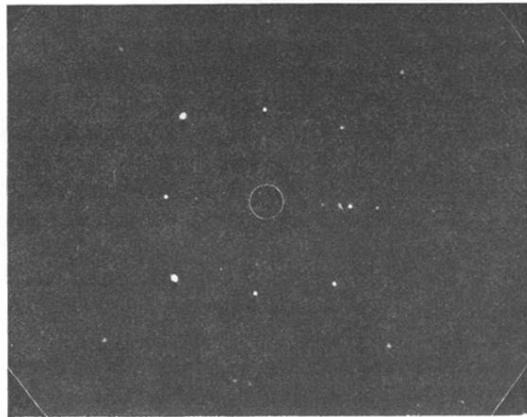


FIG. 2. X-ray back-reflection Laue pattern of a [100] single-crystal film of lead 8.4 μ thick.

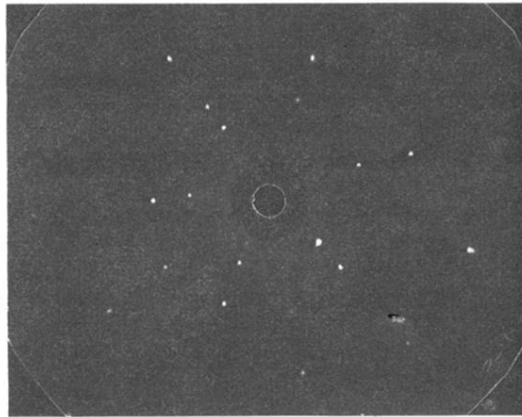


FIG. 3. X-ray back-reflection Laue pattern of a [111] single-crystal film of lead 7.3μ thick.

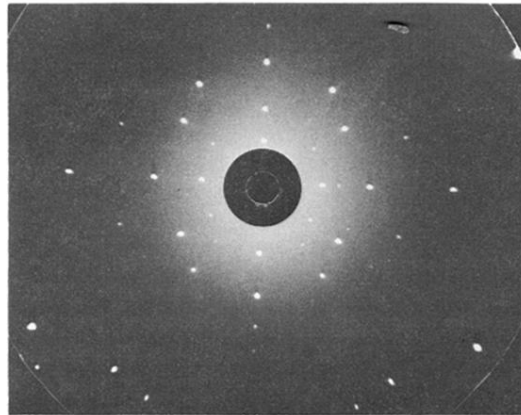


FIG. 4. X-ray back-reflection Laue pattern of a [110] single-crystal film of lead 7.0μ thick.